Physicochem. Probl. Miner. Process., 62(3), 2026, 221504

http://www.journalssystem.com/ppmp

Physicochemical Problems of Mineral Processing

ISSN 1643-1049

Property stability of ultrafine calcium hydroxide suspension prepared by wet digestion: Effect of concentration

Xinglan Li [1, 2], Xin Wang [1, 2], Wanling Zhong [3], Ming Wei [1, 2], Xiaoqin Li [4], Yahui yang [5], Kun Liu [1, 2]

[1] School of Minerals Processing and Bioengineering, Central South University, Changsha 410083, China

[2] Hunan Key Laboratory of Mineral Materials and Application, Central South University, Changsha 410083, China

[3] School of Materials and Environment, Guangxi Key Laboratory of Advanced Structural Materials and Carbon Neutralization, Guangxi Minzu University, Nanning 530105, China

[4] School of Environment and Energy, Guangdong Provincial Key Laboratory of Solid Wastes Pollution Control and Recycling, South China University of Technology, Guangzhou 510006, China

[5] College of Chemistry and Chemical Engineering, Hunan Normal University, Changsha, 410081, China

Corresponding authors. yangyahui@hunnu.edu.cn (Y. Yang), kliu@csu.edu.cn (K. Liu)

Abstract: Only the performance-stable ultrafine calcium hydroxide ($Ca(OH)_2$) suspension has industrial practical value. This study investigated the variations in particle size, morphology, crystalline phase, sedimentation, and rheological properties of three-concentration ultrafine $Ca(OH)_2$ suspensions (prepared via wet digestion) during 120 h of static settling. The results indicated that the three concentrations of ultrafine $Ca(OH)_2$ suspensions exhibited consistent patterns of change in particle size, morphology, crystalline phase, sedimentation, and rheological properties during the settling process. Firstly, particle size and morphology of $Ca(OH)_2$ only changed slightly at the initial settling stage and resumed their original states with prolonged settling. Secondly, in terms of the composition of the crystalline phase and the rheological properties, it can be observed that there is no significant change during the 120 h static settling process. Finally, regarding settling characteristics, it was found that the position of the settling interface of the ultrafine $Ca(OH)_2$ suspension was influenced by its concentration, with the settling interface of the 18.87 wt.% suspension dropping by only 8% and that of the 9.44 wt.% suspension dropping by 48%. In conclusion, the ultrafine $Ca(OH)_2$ suspension prepared by lime wet digestion showed excellent property stability and thus possesses considerable potential for industrial applications.

Keywords: ultrafine calcium hydroxide suspension, property stability, particle size and morphology, sedimentation and rheological properties

1. Introduction

The ultrafine calcium hydroxide ($Ca(OH)_2$) suspension (<10 μm) demonstrates superior performance in a wide range of applications when compared to traditional $Ca(OH)_2$ powder and other products (Asgary et al., 2011; Bastone et al., 2017; García-vera et al., 2020; Louwakul et al., 2017). In the field of medicine, when ultrafine $Ca(OH)_2$ suspension is used as a paste for root canal treatment, it can easily penetrate and fill all areas of fine and irregular dentin tubules due to its small particle size and uniform distribution. At the same time, it releases OH^- ions, making it more effective in killing bacteria and eliminating toxins compared to ordinary $Ca(OH)_2$. Additionally, it is biologically safer with fewer side effects (Kanmaz and Altunbas, 2022; Sy et al., 2021). In the field of cultural relics protection, ultrafine $Ca(OH)_2$ suspension has the advantages of a large specific surface area, high activity, fast carbonation speed, acid neutralization, and strong permeability. The degree of protection and efficiency of cultural relics is due to the ordinary $Ca(OH)_2$ (Ambrosi et al., 2001). In the field of environment, the use of ultrafine $Ca(OH)_2$ suspension to deal with acid gases (SO_2, NO_x, etc.), adsorbent, waste water treatment

DOI: 10.37190/ppmp/221504

agents, organic dyes degradation agents, etc., is significantly better than ordinary $Ca(OH)_2$ (Ha et al., n.d.; Shin et al., 2009). Furthermore, ultrafine $Ca(OH)_2$ suspension can be dispersed in aqueous silane/siloxane emulsions and subsequently sprayed onto marble surfaces, thereby imparting superhydrophobic properties to the marble (Protection, 2020). Alternatively, it can be mixed with soil and hardened to enhance the unconfined compressive strength of the soil (Yong et al., n.d.). In conclusion, ultrafine $Ca(OH)_2$ suspensions offer much higher industrial application value than ordinary $Ca(OH)_2$. Despite such superior performance, numerous experimental studies have shown that the ultrafine particle size of $Ca(OH)_2$ exhibits high reactivity and is prone to carbonization, resulting in the formation of calcium carbonate ($CaCO_3$), which affects its utilization rate (Asikin-Mijan et al., 2015; Rodriguez-Navarro et al., 2013; Samanta et al., 2016; Taglieri et al., 2014; Wang et al., 2024). Due to the slight solubility of $Ca(OH)_2$ in water, particles of $Ca(OH)_2$ in an aqueous solution undergo a process of "dissolution and recrystallization", which can easily result in changes like ultrafine $Ca(OH)_2$ suspension (Weifei, 2004; Wenli, 2021; Xin et al., 2023). Therefore, the stability of the ultrafine suspension of $Ca(OH)_2$ is directly related to its utility value.

Our previous investigations have demonstrated that ultrafine $Ca(OH)_2$ suspensions with characteristic particle size distributions (D_{10}: 0.303 μm, D_{50}: 1.750 μm, D_{90}: 4.534 μm) can be efficiently prepared through a wet lime digestion process without requiring chemical additives (Wang et al., 2024). This additive-free preparation strategy presents distinct advantages for industrial scale-up and practical application: first, it realizes excellent environmental friendliness by avoiding the introduction of exogenous chemical additives, thus preventing secondary pollution from additive residues in the suspension and complying with the core requirements of green chemical engineering and environmental engineering applications, such as acid gas adsorption and organic dye degradation in wastewater. Second, the absence of additive residues ensures the high chemical purity and reactivity of the ultrafine $Ca(OH)_2$ suspension, making it particularly suitable for application fields with stringent purity demands, including medical root canal treatment and cultural relics protection. Third, the process simplifies industrial operation by omitting the additional steps of additive feeding, separation, and purification, which effectively reduces the investment in production equipment and raw material costs and enables facile large-scale industrial promotion and application. Despite this advancement, many industrial applications continue to rely on direct powder addition due to practical limitations in implementing on-site suspension preparation systems. This conventional approach significantly compromises the performance benefits achievable with well-dispersed suspensions.

The critical need to understand the stability mechanisms of ultrafine $Ca(OH)_2$ suspensions becomes evident when considering their widespread industrial applications. A comprehensive evaluation of suspension stability - encompassing particle size distribution, morphological characteristics, crystalline phase integrity, and sedimentation behavior - is essential for optimizing production protocols, storage conditions, and end-use performance. Existing studies have mainly focused on the preparation of ultrafine $Ca(OH)_2$ suspension or the stability of a single performance, but a few studies have systematically explored the synergistic variation law of particle size, crystalline phase, sedimentation, rheology, and other properties of the suspension during static settling under different solid concentrations, nor have they clarified the regulation mechanism of concentration on the comprehensive stability of the suspension. In addition, there is a lack of experimental data on the long-term static performance evolution of ultrafine $Ca(OH)_2$ suspension prepared by wet digestion at different concentrations.

Based on the above considerations, the present study focuses on the ultrafine $Ca(OH)_2$ prepared via the wet lime digestion method in our previous work. We systematically investigate the changes in physicochemical properties (i.e., particle size, morphology, crystalline phase, and sedimentation behavior) of these suspensions during 120 h of static settling in 50 cm^3 measuring cylinders. In addition, $Ca(OH)_2$ suspension is the macroscopic uniform dispersion of $Ca(OH)_2$ particles in water, which can be regarded as a fluid (Atzeni et al., 2004). Changes in its rheological properties can not only explain the potential impact on application, but also indirectly reflect changes in the property stability of the suspension. Therefore, we also investigated the rheological changes of the suspension during the static settling process. This study fills this gap by systematically investigating changes in the physicochemical properties of three concentrations of an ultrafine $Ca(OH)_2$ suspension during 120 h of static settling,

revealing the regulatory effect of solid concentration on suspension stability, and providing theoretical and data support for the industrial application of the suspension.

2. Materials and methods

2.1. Materials

Lime (94% CaO) was supplied by Guangxi Xiayang Environmental Protection Technology Co., and deionized (DI) water (resistivity 18.25 MΩ ·cm) was prepared using a QQUP20W water purifier.

The quick lime was analyzed using X-ray fluorescence spectroscopy (XRF) and scanning electron microscopy (SEM (Table 1 and Fig. 1).

As shown in Table 1 and Fig. 1, the raw material used in this study is off-white quicklime blocks with a particle size of approximately 2 cm. Its main components are calcium (Ca) and oxygen (O), with only trace amounts of silicon (Si) and titanium (Ti) present (totaling 0.25% by weight). The primary component phases consist of calcium oxide (CaO), along with small quantities of calcite-type $CaCO_3$ and $Ca(OH)_2$ (resulting from the reaction between quicklime storage, carbon dioxide, and moisture in the air).

Table 1. Composition of lime (wt.%)

Ingredient	CaO	SiO_2	TiO_2
quicklime	95.13	0.47	0.05

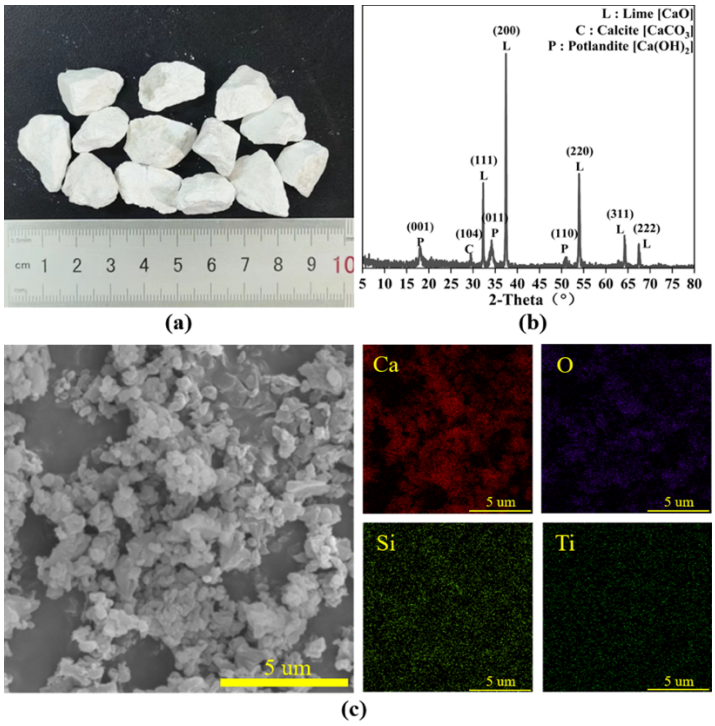

Fig. 1. Optical photographs of lime (a), XRD image (b), SEM and EDS analysis (c)

2.2. Methods

2.2.1. Preparation of ultrafine calcium hydroxide suspension

Following our previous method (Wang et al., 2024), 10 g of lime with a particle size ranging from 900-2000 μm was added into a 250 cm^3 conical flask containing 60 cm^3 of DI water at a constant temperature of 60 ˚C in a water bath, and the digestion reaction was then conducted for a duration of 40 min under magnetic stirring at 400 rpm. After the end of the reaction, ultrafine $Ca(OH)_2$ suspension with particle size distributions D_{10}, D_{50}, and D_{90} of 0.303, 1.750, and 4.534 μm and concentration of 18.87 wt.% was obtained. In addition, weigh 35 g and 25 g ultrafine $Ca(OH)_2$ suspension with a concentration of 18.87

wt.%, dilute to 50 g with water, respectively, and then shake well to prepare two ultrafine $Ca(OH)_2$ suspensions. The former is an ultrafine $Ca(OH)_2$ suspension with particle size distributions D_{10}, D_{50}, and D_{90} of 0.297, 1.549, and 4.392 μm, and a concentration of 13.21 wt.%. The latter is an ultrafine $Ca(OH)_2$ suspension with particle size distributions D_{10}, D_{50}, and D_{90} of 0.288, 1.382, and 4.317 μm, and a concentration of 9.44 wt.%. The three concentrations were selected based on three key considerations: (1) Industrial relevance: they fully cover the typical 5–20 wt.% concentration range used in industrial wet digestion processes, with 18.87 wt.% being the original optimized product; (2) Scientific gradient: the ~5 wt.% step difference clearly reflects the property variation trend with concentration; (3) Pre-experimental validation: this gradient generates statistically significant differences in sedimentation and rheological properties.

Study on the property stability of ultrafine $Ca(OH)_2$ suspension: The above three concentrations of ultrafine $Ca(OH)_2$ suspension were measured 50 cm^3 each into a measuring cylinder of the same specifications (the cylinder was the cylinder was tightly wrapped with polytetrafluoroethylene (PTFE) sealing film, then sealed with a rubber stopper, and finally wrapped with waterproof adhesive tape on the outside of the rubber stopper) and allowed to static settling for 120 hours at 25 ˚C. During the static settling process, the position of the settling interface of the suspension of different concentrations was recorded by taking photos, and the settlement curve was drawn. In addition, the suspensions of 0 h, 24 h, 48 h, 72 h, 96 h, and 120 h were shaken and dispersed uniformly; the particle size, morphology, and crystalline phase were characterized after drying the dispersed suspension, while the rheological property was measured directly on the well-dispersed wet suspension.

2.2.2. Determination of calcium hydroxide content

The determination method for $Ca(OH)_2$ content in the preparation of $Ca(OH)_2$ samples follows the industrial standard HG/T 4120-2009 for determining $Ca(OH)_2$ content. The method involves adding a sucrose solution to react with the $Ca(OH)_2$ solution, resulting in the formation of calcium sucrose. Phenolphthalein is used as an indicator, and the content of $Ca(OH)_2$ is calculated by titration with a hydrochloric acid solution until it becomes colorless using Eq. (1):

$$\omega = \frac{(V-V0)/1000\times c\times M}{m}\times 100\% \quad (1)$$

where ω is calcium hydroxide content (%), c is the concentration of the standard titration solution of hydrochloric acid (mol/dm^3), V is the volume of hydrochloric acid consumed by the experimental solution (cm^3), V_0 is the volume of hydrochloric acid consumed by blank solution (cm^3), m is the numerical value of the mass of the sample (g), M is the value of the molar mass of calcium hydroxide [1/2$Ca(OH)_2$] (g/mol) (M=37.05).

The specific concentrations of the solutions used were 300 g/dm^3 sucrose solution, 4 g/dm^3 sodium hydroxide solution, 10 g/dm^3 phenolphthalein solution, and 0.5002 mol/dm^3 hydrochloric acid standard titration solution.

2.2.3. Analytical techniques

The particle size of $Ca(OH)_2$ suspension was measured using a BT-9300ST laser particle size distribution analyzer by dispersing it in ethanol. The morphology of $Ca(OH)_2$ suspension was characterized by a JSM-7900F field emission scanning electron microscopy (FESEM). The crystal structure of $Ca(OH)_2$ was determined using a TD-3500 XRD diffractometer with a scanning range of 5 - 80 ˚ (2θ) and a scanning speed of 0.02 ˚/s. The rheological property of $Ca(OH)_2$ suspension was measured using the MCR 102 modular intelligent advanced rheometer in "viscosity and flow curve (V2.0)" mode, with measurements conducted at a controlled temperature of 25 ˚C.

3. Results and discussion

3.1. Characterization of ultrafine calcium hydroxide suspension

As shown in Fig. 2, the particle size distribution of the prepared ultrafine $Ca(OH)_2$ suspension indicates that most of the particles (94.82%) are distributed below 5 μm, but the distribution is not uniform throughout.

Furthermore, Fig. 3 reveals that there is severe agglomeration between particles in the prepared ultra-fine $Ca(OH)_2$ suspension, primarily caused by particles with a size of about 100 nm aggregating together. Additionally, our previous research paper's XRD results demonstrate that the ultrafine $Ca(OH)_2$ suspension mainly consists of $Ca(OH)_2$ with a small amount of $CaCO_3$; titration analysis shows that the content of $Ca(OH)_2$ is 93.86%.

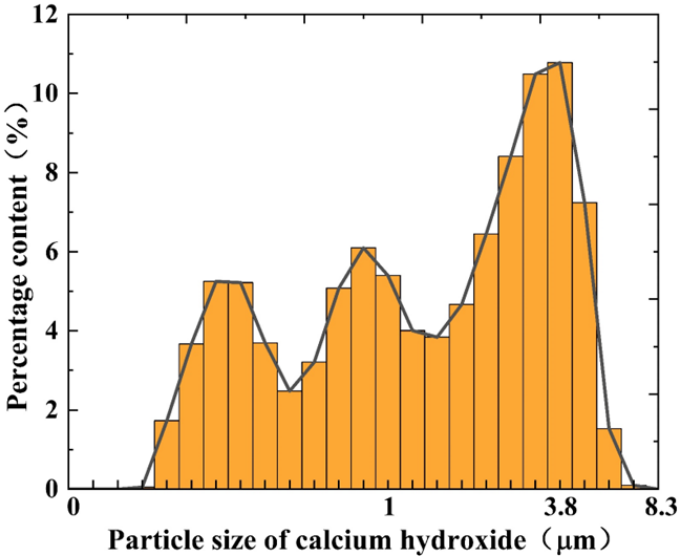

Fig. 2. Particle size distribution of ultrafine $Ca(OH)_2$ suspension

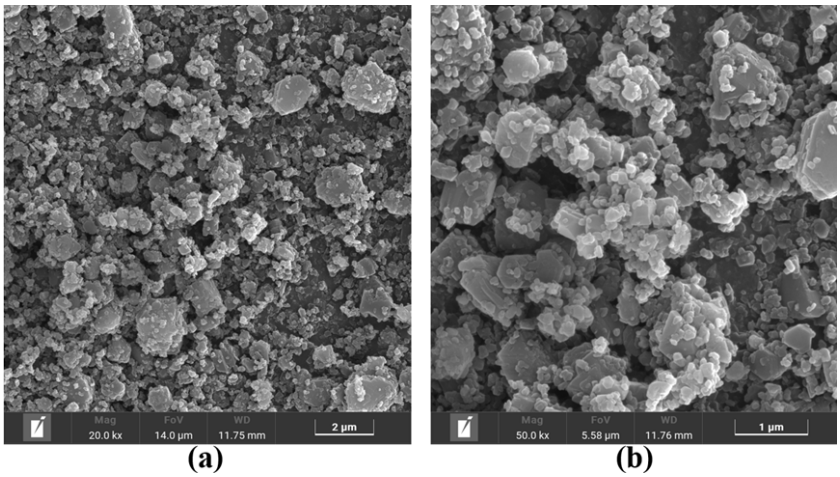

Fig. 3. SEM photograph of $Ca(OH)_2$ particles in ultrafine $Ca(OH)_2$ suspension: (a) 20,000× magnification, (b) 50,000× magnification

3.2. Changes in particle size and morphology

The particle size and morphology are crucial parameters for characterizing the properties of ultrafine $Ca(OH)_2$ suspension. Due to the nature of $Ca(OH)_2$ slightly soluble in water, $Ca(OH)_2$ particles undergo a "dissolution and recrystallization" process in aqueous solutions, which can easily lead to changes in both particle size and morphology (Weifei, 2004; Wenli, 2021; Xin et al., 2023). Therefore, it is imperative to investigate the changes in particle size and morphology of ultrafine $Ca(OH)_2$ suspension during the static settling process to examine the property stability of the suspension.

3.2.1. Changes in particle size

The initial particle sizes of $Ca(OH)_2$ suspension with concentrations of 18.87 wt.%, 13.21 wt.%, and 9.44 wt.% are summarized in Table 2. It can be seen from Fig. 3(a, b) and Table 1 that the three

suspensions are all ultrafine $Ca(OH)_2$ suspensions. Furthermore, a decrease in concentration is accompanied by a reduction in particle size within the suspensions.

The ultrafine $Ca(OH)_2$ suspension of the above three concentrations was placed at 25 ˚C in a 50 cm^3 measuring cylinder for 120 h static settling process. During this process, the particle size of the suspension was measured at intervals of 24 h to observe any changes in particle size. The experimental results are presented in Fig. 4.

Table 2. Initial particle size of $Ca(OH)_2$ suspension with different concentrations

Concentration (wt.%)	Particle size of $Ca(OH)_2$ suspension (μm)		
	D_{10}	D_{50}	D_{90}
18.87	0.303	1.750	4.534
13.21	0.297	1.549	4.392
9.44	0.288	1.382	4.317

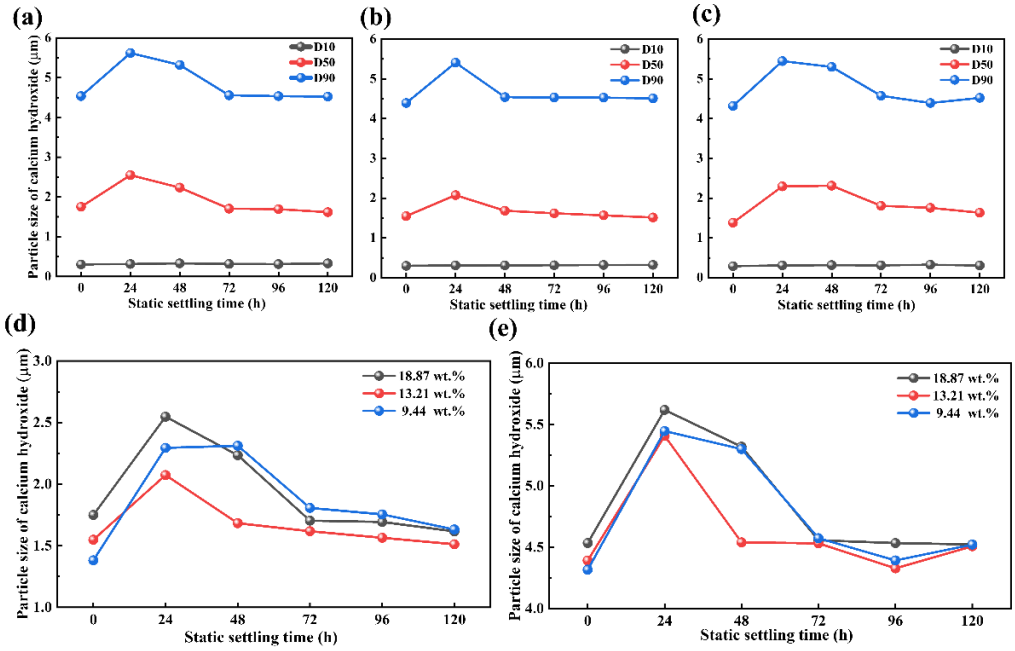

Fig. 4. Particle size change of ultrafine $Ca(OH)_2$ suspensions with different concentrations within 120 h static settling time: (a)18.87 wt.%, (b) 13.21 wt.%, (c) 9.44 wt.%; Influence of different ultrafine $Ca(OH)_2$ suspension concentration on particle size D_{50} (d) and D_{90} (e) within 120 h static settling time

As depicted in Figs. 4(a–c), the particle size of the ultrafine $Ca(OH)_2$ suspension at all three concentrations exhibits regular changes with increasing static settling time. With the extension of the settling time, the particle size parameters (D_{10}, D_{50}, and D_{90}) initially increase and then decrease, and reaches its maximum at a static settling time of 24 h. However, it should be noted that the particle size does not exceed 10 μm, as indicated in Table 3. Furthermore, Fig. 1 reveals that the reduction in particle size of the three concentration suspensions diminishes significantly and gradually becomes more uniform after a static settling period of 72 h. Moreover, the particle size reaches equilibrium with minimal deviation from the initial particle size.

Table 3. Particle size of ultrafine $Ca(OH)_2$ suspension with different concentrations after 24 h of static settling

Concentration (wt.%)	Particle size of $Ca(OH)_2$ suspension (μm)		
	D_{10}	D_{50}	D_{90}
18.87	0.313	2.548	5.619
13.21	0.308	2.074	5.408
9.44	0.308	2.295	5.447

The particle size increase in the first 24 h of static settlement may be due to the unstable state of the system at this time. To make the system reach the minimum internal energy, small crystals with high internal energy will dissolve and crystallize on the large crystals, increasing the particle size of $Ca(OH)_2$ (Mascolo et al., 2010, 2017). The reduction of $Ca(OH)_2$ particle size after 24 h and the weakened reduction trend after 72 h have resulted from the dissolution of $Ca(OH)_2$ crystal when it grew to a certain size, and the crystal dissolution rate is greater than the recrystallization rate. However, this process will be weakened with the extension of static settling time, so the $Ca(OH)_2$ particle size will eventually stabilize at a small value (Adamson, 1960; Bohá and Ne, 2016; Rodriguez-navarro et al., 1998; Wenli, 2021).

To explore the influence of the concentration of ultrafine $Ca(OH)_2$ suspension on particle size, the D_{50} and D_{90} data of suspension with different concentrations were summarized and plotted into a graph (D_{10} data were not used as a reference because the values were too small and the measurement errors were relatively large), as shown in Figs. 4(d) and (e).

As shown in Figs. 4(d) and (e), the concentration of ultrafine $Ca(OH)_2$ suspension has a regular effect on the particle size when the suspension is allowed to static settling for the same time, with 13.21 wt.% as the critical concentration: the particle size gradually decreases when the concentration reduces from 18.87 wt.% to 13.21 wt.%, while the particle size increases instead when the concentration further reduces from 13.21 wt.% to 9.44 wt.%. The reason for this phenomenon may be that when the concentration is high, the spacing between $Ca(OH)_2$ particles is small, and the $Ca(OH)_2$ particles tend to aggregate, increasing in $Ca(OH)_2$ particle size **Błąd! Nie można odnaleźć źródła odwołania.,Błąd! Nie można odnaleźć źródła odwołania.**. However, when the concentration is excessively reduced (below 13.21 wt.%), the amount of dissolved $Ca(OH)_2$ in the aqueous solution of the system increases, and the "dissolution and recrystallization" process of $Ca(OH)_2$ particles is intensified, increasing in particle size. Therefore, a suspension with a smaller particle size can be obtained by appropriately reducing the suspension concentration to around 13.21 wt.%, while excessive concentration reduction will lead to the reverse increase of particle size.

3.2.2. Changes in morphology

Three concentrations of ultrafine $Ca(OH)_2$ suspensions were taken and allowed to static settling for 0, 24, 48, 72, 96, and 120 h, respectively. The changes in particle morphology during the static settling were observed, as shown in Fig. 5.

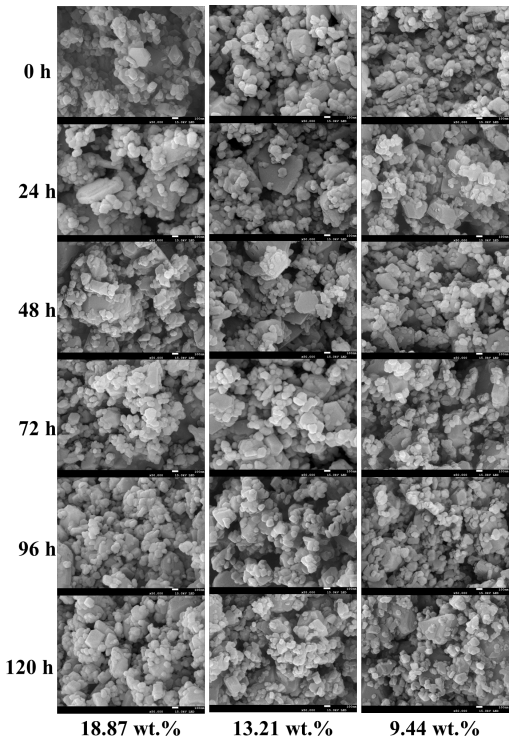

Fig. 5. Changes in particle morphology of ultrafine $Ca(OH)_2$ suspension with different concentrations after static

settling for different times (0, 24, 48, 72, 96, and 120 h)

Figs. 6(a-c) demonstrate that the morphologies of the ultrafine $Ca(OH)_2$ suspension particles at three concentrations all change significantly with the extension of the static settling time, but the fully regular hexagon-shaped plates do not appear as described (Darroudi et al., 2016; Dhanuskodi and Prabukumar, 2017). In this experiment, the morphology of $Ca(OH)_2$ particles is mainly an irregular small polyhedron.

This is because the calcined lime used in this experiment is in small, irregular polyhedron pieces, and the particles are immediately broken during the digestion process, which accelerates the formation process of hydrogel on the surface of the $Ca(OH)_2$ crystals, and also accelerates the transformation process of the $Ca(OH)_2$ crystals from regular crystals to smaller, irregular crystals (Mascolo et al., 2017). In addition, from the overall particle size of the particles in the SEM images, it can be found that when the static settling time is 0 h, the ultra-fine $Ca(OH)_2$ suspension with a lower concentration has a significantly smaller particle size. The particle size increases significantly after 24 h of static settlement, but decreases during 24 ~ 72 h of static settlement. There is no significant change in particle size when the settling time continues to extend. This is basically consistent with the data from the laser particle size analyzer.

3.3. Changes in crystalline phase

In the process of static settling, the "dissolution-recrystallization" behavior of $Ca(OH)_2$ crystals will also affect the crystalline phase of $Ca(OH)_2$, so the crystalline phase change of ultrafine $Ca(OH)_2$ suspension can also reflect its property stability to a certain extent. The above three concentrations of ultrafine $Ca(OH)_2$ suspensions with static settling times of 0, 24, 48, 72, 96, and 120h were respectively taken to analyze by XRD, as shown in Fig. 6.

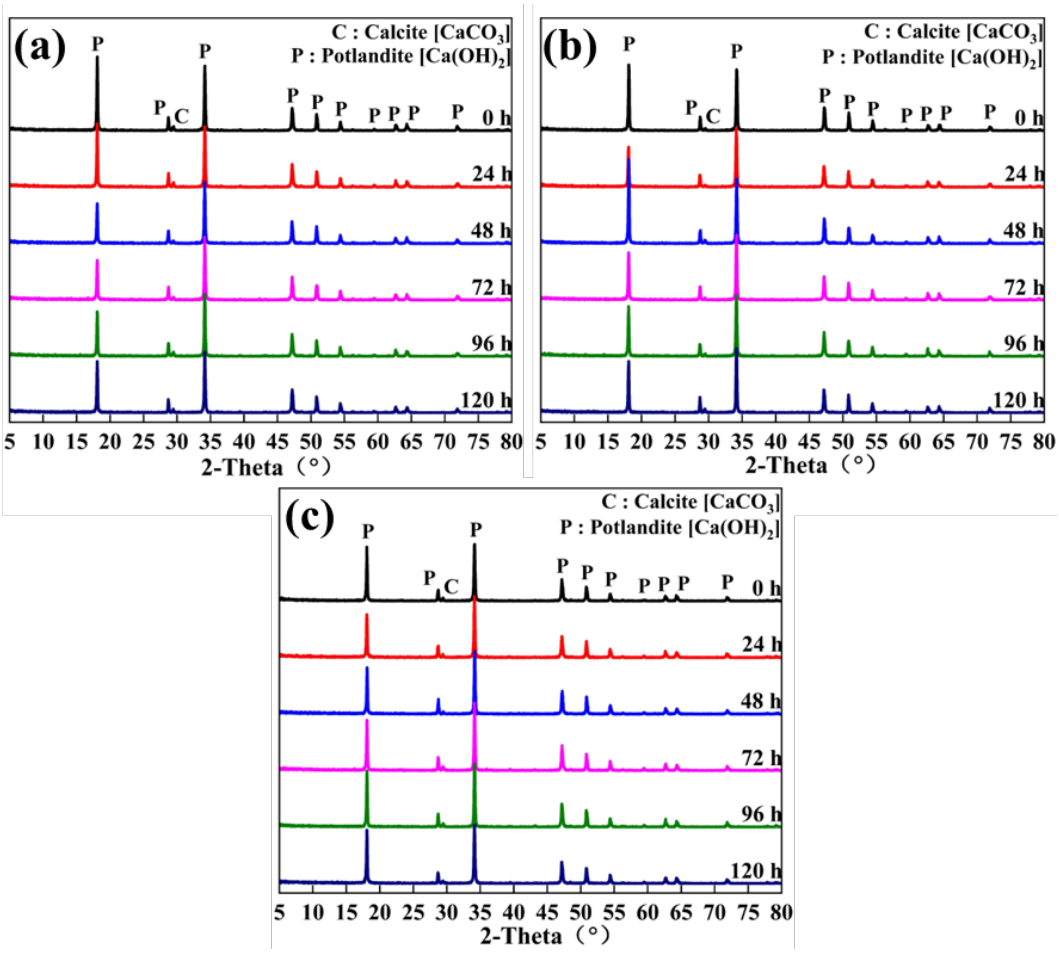

Fig. 6. XRD patterns of ultrafine $Ca(OH)_2$ suspensions with different concentrations and static settling times: (a)18.87 wt.%, (b) 13.21 wt.%, (c) 9.44 wt.%

As shown in Fig. 6, after static settling for different times, the crystalline phase composition of different ultrafine $Ca(OH)_2$ suspensions with different concentrations is mainly $Ca(OH)_2$ with a small amount of $CaCO_3$. The results of quantitative analysis show that the content of $Ca(OH)_2$ in each sample does not change significantly, indicating that the composition of the crystalline phase in different suspensions does not change significantly under sealed conditions. However, a closer look at the XRD patterns shows that the intensity of the diffraction peaks at 18.00 °, 28.47 °, and 34.10 ° varies greatly during the settling process. This shows that the (001), (100), and (101) crystal faces of the $Ca(OH)_2$ crystals change significantly during the static settling process. According to relevant research (001), the crystal face of $Ca(OH)_2$ has the lowest surface energy and the slowest growth rate (Adamson, 1960; Bohá and Ne, 2016; Rodriguez-Navarro et al., 1998; Wenli, 2021). During the static settling process, to achieve the lowest internal energy, the (100) and (101) crystal faces of $Ca(OH)_2$ particles will gradually dissolve, thus promoting the growth of the (001) crystal face (Adamson, 1960; Bohá and Ne, 2016; Rodriguez-navarro et al., 1998; Wenli, 2021). Therefore, for the ultrafine $Ca(OH)_2$ suspension of different concentrations, the progress of the static settling process is expressed by dividing the peak area of (001) crystal face by the sum of the peak areas of (100) and (101) crystal faces, namely peak area ratio (PAR). A lower value indicates that fewer (001) faces are generated, and vice versa. The calculated results are shown in Fig. 6.

As seen from Fig. 8, with the extension of static settling time, the peak area ratios (PAR) show a law of first decreasing and then increasing. This is because, as the surface with the lowest crystal face energy of $Ca(OH)_2$, the (001) crystal face grew slowly. The dissolution and recrystallization of smaller particle crystals in the initial stage of static settling results in a much slower formation rate of the (001) crystal face compared to the (100) and (101) crystal faces, leading to a decrease in the PAR. However, with the extension of static settling time, the system gradually stabilizes and tends to form (001) crystal face, increasing PAR. This is consistent with the above research results. In addition, it is seen from Fig. 6 that $Ca(OH)_2$ concentration also has a certain influence on the formation of crystal faces. At the initial stage of static settling, the mass transfer resistance of the high concentration system is high, the dissolution and crystallization behavior of $Ca(OH)_2$ crystal is weak, and the (001) crystal faces are well developed. With the extension of the static settling time, the mass transfer resistance of the low concentration system is small, and the formation speed of (001) crystal faces is faster, so the PAR is higher than that of the high concentration system.

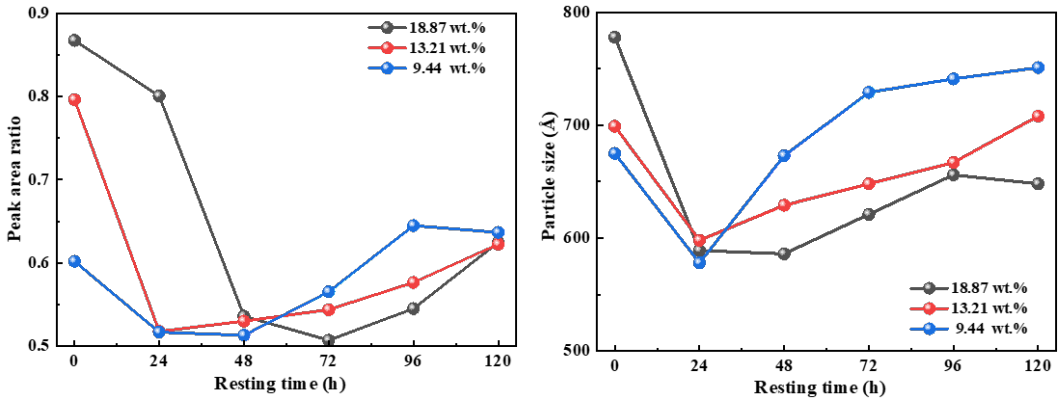

Fig. 7. The change of PAR(a) and particle size(b) with static settling time at different concentrations of ultrafine $Ca(OH)_2$ suspension

The average particle size of $Ca(OH)_2$ is calculated by using MDI JADE 6 software, as shown in Figs. 7(a) and (b). With the extension of static settling time, the average particle size of $Ca(OH)_2$ first decreases and then increases. In addition, the average particle size of the high concentration system is larger at the early stage of static settling, while that of the low concentration system is larger at the later stage of static settling. This is consistent with the above influence law and mechanism of the PAR. In the early stage of static settling, the dissolution and recrystallization behavior of $Ca(OH)_2$ crystals is obvious; the dissolution reduces the particle size, and the particle size formed by crystallization in solution is also small. At the later stage of static settling, the particle size increases. The high concentration system has

strong mass transfer resistance, which hinders the dissolution, formation, and growth of particles, so the above results appear.

The above crystal growth behavior and crystalline phase stability have important guiding significance for the industrial application of ultrafine $Ca(OH)_2$ suspensions. In the field of industrial environmental protection, the preferential growth of the (001) crystal plane increases the specific surface area and surface reactivity of $Ca(OH)_2$ particles, which significantly enhances their adsorption capacity and reaction rate for acid gases (SO_2, NO_x) and organic pollutants in industrial wastewater. This can effectively reduce the dosage of reagents and operating costs in industrial flue gas desulfurization and denitrification, as well as printing and dyeing wastewater treatment. Meanwhile, the stable crystalline phase composition ensures that the suspension maintains high reactivity during industrial storage and transportation, avoiding performance degradation caused by crystal phase transformation.

3.4. Changes in sedimentation property

The stability of the ultrafine $Ca(OH)_2$ suspension can be described by the sedimentation rate during the static settling period(Kitamura et al., 2002; Lanzón et al., 2023; Navrátilová et al., n.d.). During the static settling of suspension, the settling velocity of the suspension was described by photographing the position of the settling interface, as shown in Table 4 and Figs. 8(a), (b), and (c).

Table 4. The sedimentation interface height of ultrafine $Ca(OH)_2$ suspension under different static settling times

Static settling times (h)	Numerical values of settling interface (cm^3)		
	18.87 wt.%	13.21 wt.%	9.44 wt.%
0	50.0	50.0	50.0
24	48.7	46.7	35.0
48	47.7	43.2	28.0
72	47.0	41.0	25.5
96	46.5	39.7	24.4
120	46.0	38.8	24.0

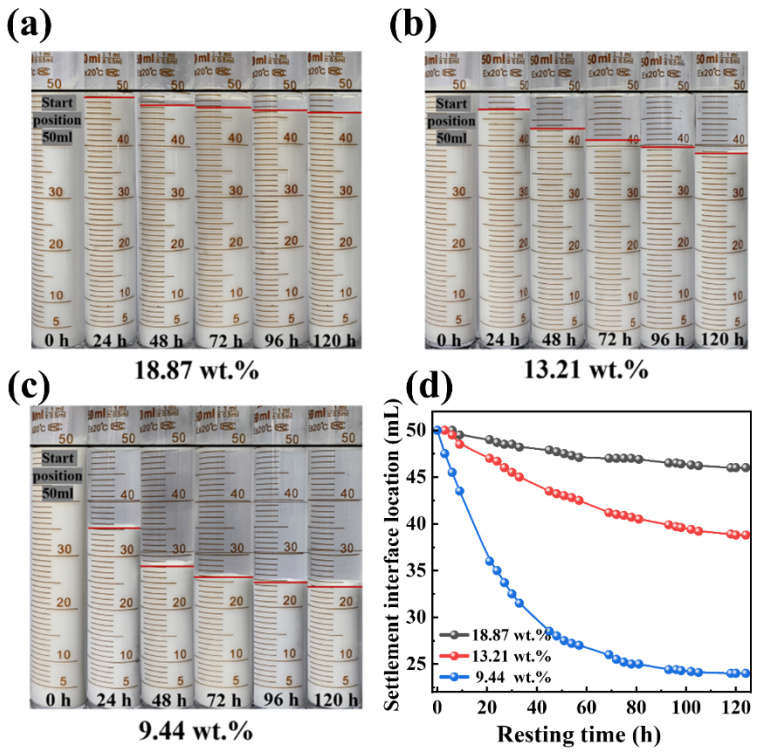

Fig. 8. The change of settling interface with static settling time at different concentrations of ultrafine $Ca(OH)_2$ suspension (a) - (c); Sedimentation curve of ultrafine $Ca(OH)_2$ suspension with different concentrations (120h)

According to the above methods, the sedimentation interface height of $Ca(OH)_2$ suspension within 120 h of static settling was recorded, and the sedimentation curves of the three kinds of suspension with different concentrations were plotted, as shown in Fig. 8(d).

It is seen from Fig. 8(d) that all three ultrafine $Ca(OH)_2$ suspensions precipitate within 120 h of settling, especially within 72 h of static settling, and the suspensions precipitate rapidly. There is always a clear $Ca(OH)_2$-water interface during sedimentation. Obviously, the lower the concentration of suspension, the more obvious the settling effect. For suspensions with concentrations of 9.44 wt.%, 13.21 wt.%, and 18.87 wt.%, the proportion of settling height is 52%, 22.4%, and 8%, respectively. This phenomenon shows that the ultra-fine $Ca(OH)_2$ suspension with a higher concentration has better settling stability and can be placed for a longer time, which is conducive to the use of an industrial scale.

Sedimentation behavior of the suspension is essentially governed by particle size and interparticle interactions, and the coupling effect of these two factors leads to the seemingly contradictory results between particle size characteristics (Section 3.2.1) and sedimentation rate in this study. At 24 h of static settling, the 18.87 wt.% suspension exhibited the largest D_{50} value among the three concentrations (Fig. 4d), which would theoretically result in the highest gravitational sedimentation rate. However, the high solid concentration of the 18.87 wt.% suspension induced strong van der Waals and electrostatic interactions between particles; the aggregated particles further formed a continuous three-dimensional spatial network structure in the aqueous phase. This network structure generated significant steric hindrance to the downward movement of particles under gravity, which completely offset the gravitational sedimentation effect caused by the large particle size, thus leading to the lowest sedimentation rate of the 18.87 wt.% suspension.

After 72 h of static settling, the particle sizes (D_{50} and D_{90}) of the three concentration suspensions tended to be stable and were close to each other (Figs. 4d and 4e), but the sedimentation curves still showed a significant difference (Fig. 8d). This is because the spatial network structures formed by particles in suspensions with different concentrations remained essentially different even when the particle sizes were similar. For the low-concentration suspensions (9.44 wt.% and 13.21 wt.%), the sparse particle distribution led to a loose and discontinuous spatial network structure, where the interparticle steric hindrance was extremely weak. Under this condition, gravitational sedimentation became the dominant factor for particle movement, resulting in a continuous decrease in the settling interface. In contrast, the high-concentration 18.87 wt.% suspension maintained a relatively compact and continuous spatial network structure due to the high particle packing density, which still effectively inhibited the sedimentation of $Ca(OH)_2$ particles. Therefore, even with similar particle sizes after 72 h, the sedimentation behavior of the suspensions still showed a significant concentration dependence, which further confirmed that solid concentration is a key regulatory factor for the sedimentation stability of ultrafine $Ca(OH)_2$ suspensions.

3.5. Changes in rheological property

The rheological properties of $Ca(OH)_2$ suspensions are critical for their practical applications, including lime-based protective repair materials, binders, and lime mortar, where rheological behavior is a key performance parameter (Aggelakopoulou et al., 2019; Arizzi, 2019; Navratilova and Nedela, n.d.). Many studies have proved that the rheological property of $Ca(OH)_2$ suspension is closely related to its microstructure (Atzeni et al., 2004; Romero-Hermida et al., 2019; Ruiz-Agudo and Rodriguez-Navarro, 2010). According to the above experimental results, the particle size, morphology, and crystal phase of $Ca(OH)_2$ have changed to different degrees during the static settling process, which will inevitably affect the rheological properties of the suspension. Therefore, kinematic viscosity curves of three kinds of ultrafine $Ca(OH)_2$ suspensions with different static settling times were measured, as shown in Fig. 9.

As seen from Figs. 9(a), (b), and (c), the viscosity of all ultrafine $Ca(OH)_2$ suspensions shows an obvious decreasing trend with the increased in shear rate, indicating that they are all shear-thinning fluids (Anqi and Dingyi, 2020). The linear fitting is performed on the above data, and the trend law is consistent with the power-law fluid model(Huimin, 2013). The power-law fluid model is expressed as follows (Huimin, 2013):

$$\eta = k\gamma^{n-1} \tag{2}$$

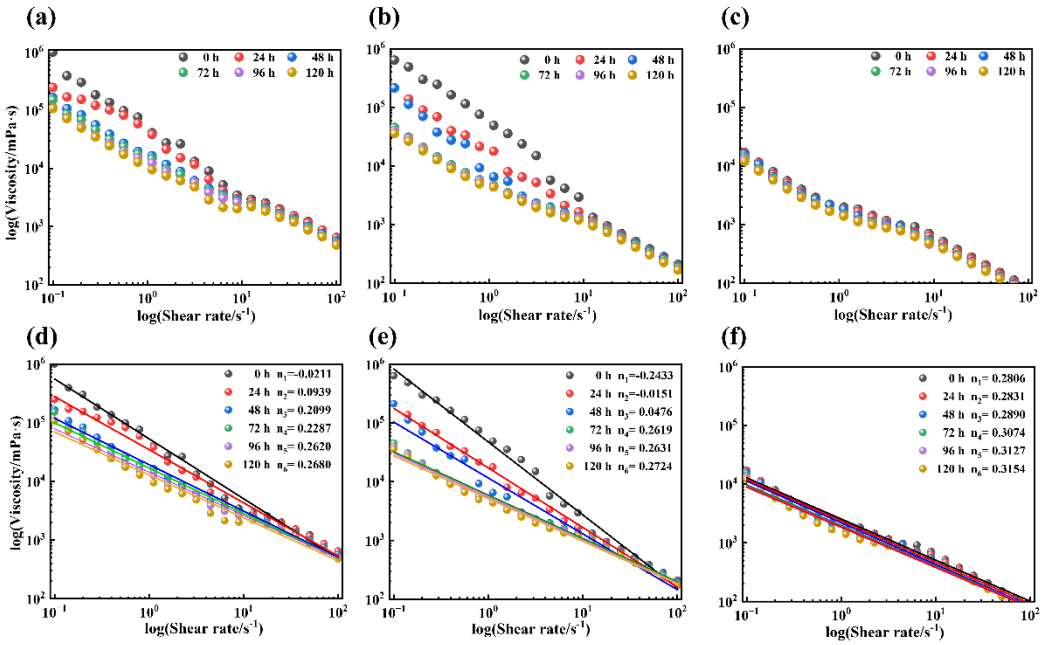

Fig. 9. Kinematic viscosity curves and fitting curves of different concentrations of ultrafine $Ca(OH)_2$ suspensions at different static settling times: (a) and (d) 18.87 wt.%, (b) and (e) 13.21 wt.%, (c) and (f) 9.44 wt.%

where η is the viscosity （Pa·s, γ is the shear rate （s^{-1}), k is the consistency index, also known as the viscosity coefficient, which is a measure of viscosity but is not equal to the viscosity value. Generally, the larger the viscosity, the larger the value of n is the power law exponent; the greater the deviation of n from 1, the stronger the non-Newtonian nature of the fluid; when n < 1, the power law equation reflects the pseudoplastic fluid with shear thinning.

Eq. (2) can be written as Eq. (3) by transformation:

$$\lg \eta = \lg k + (n-1)\lg\gamma \tag{3}$$

The experimental data are fitted according to Eq. (3), and the fitting linear correlation coefficient R^2 is shown in Table 5. The fitting experimental results are shown in Table 5 and Fig. 9(d), (e), and (f).

Table 5. Fitting linear correlation coefficients R^2 of ultrafine $Ca(OH)_2$ suspension with different concentrations and static settling times

Concentration	Fitting linear correlation coefficients at different static settling times points, R^2					
(wt.%)	0 h	24 h	48 h	72 h	96 h	120 h
18.87	0.9867	0.9863	0.9907	0.9903	0.9920	0.9805
13.21	0.9925	0.9957	0.9710	0.9913	0.9921	0.9922
9.44	0.9863	0.9879	0.9891	0.9560	0.9866	0.9874

Table 6. The logarithm of the consistency coefficient of the s ultrafine $Ca(OH)_2$ suspension with different concentrations when static settling for different times

Concentration	The logarithm of the consistency coefficient at different static settling times (lgk)					
(wt.%)	0 h	24 h	48 h	72 h	96 h	120 h
18.87	4.73	4.54	4.29	4.18	4.16	4.14
13.21	4.68	4.24	4.06	3.77	3.74	3.72
9.44	3.41	3.38	3.34	3.29	3.28	3.27

As seen from Table 5, the fitting correlation coefficients R^2 are mostly above 0.98, indicating that the three kinds of suspensions basically conform to the power law fluid model as a fluid. As can be seen from Fig. 9 and Table 6, all suspensions are pseudoplastic fluid that thins under shear. With the

extension of static settling time, the non-Newtonian nature of the suspension at the same concentration weakens, and the consistency shows a decreasing trend. After static settling for 72 h, the range of change decreases. This is because of the agglomeration of $Ca(OH)_2$ particles (Atzeni et al., 2004; Romero-Hermida et al., 2019; Ruiz-Agudo and Rodriguez-Navarro, 2010; Wenli, 2021). Within 0-24 h static settling, the particle size of $Ca(OH)_2$ increases, which makes the particle agglomerate size increase and the viscosity decrease. Then, the particle size of $Ca(OH)_2$ decreases gradually after static settling for 24-72 h, and the agglomeration phenomenon is intensified. With the increase in the number of $Ca(OH)_2$ particles in the aggregates, the particle size of the aggregates further increases, and the viscosity further decreases. However, after 72 h of static settling, the system gradually reaches the most stable state, and the viscosity gradually becomes constant (Atzeni et al., 2004; Romero-Hermida et al., 2019; Ruiz-Agudo and Rodriguez-Navarro, 2010; Wenli, 2021).. In addition, the viscosity of the high-concentration ultrafine $Ca(OH)_2$ suspension is also relatively large, which is consistent with the experimental phenomenon and the reported research results (Wenli, 2021).

4. Conclusions

The stability of ultrafine calcium hydroxide ($Ca(OH)_2$) suspension is an important index to judge its value and use. This present study mainly investigates the changes in particle size, morphology, crystalline phase, sedimentation, and rheological properties of the ultrafine $Ca(OH)_2$ suspension prepared by lime wet digestion method during the 120 h static settling process in a 50 cm^3 measuring cylinder. The results show that the particle size, morphology, crystalline phase, sedimentation, and rheological properties of the suspension are changed to some extent by the dynamic process of "dissolution and recrystallization" of $Ca(OH)_2$ particles. The particle size and morphology only changed to a certain extent at the beginning of static settling, but the degree of change was small, and continued static settling would result in the particles returning to their initial size. Notably, the crystalline phase composition remained unchanged (dominated by $Ca(OH)_2$ with minor $CaCO_3$), while the (001) crystal plane exhibited significant preferential growth. This crystal characteristic, combined with stable rheological properties, endows the suspension with excellent industrial performance in environmental protection, geotechnical engineering, and building materials. The high concentration ultrafine $Ca(OH)_2$ suspension (18.87 wt.%) has a certain stability of settling within 120 h, and a large degree of settling phenomenon will not occur in a short time. In summary, the prepared ultrafine $Ca(OH)_2$ suspension (18.87 wt.%) has certain property stability within 120 h. Therefore, it is proven that the ultrafine $Ca(OH)_2$ suspension prepared by the wet digestion process of lime has certain property stability in a short time, which plays an important guiding significance for the preparation of ultrafine $Ca(OH)_2$ suspension with stable properties by the wet digestion process of lime in industry, as well as the storage and use of the suspension.

Acknowledgments

This work was supported by the National Key Research and Development Program of China under Grant No. 2022YFC3900905, and the Hunan Provincial Key Research and Development Program under Grant No. 2025JK2075.

References

ADAMSON, A.W., 1960. Physical chemistry of surfaces. (doi.org/10.1149/1.2133374)

AGGELAKOPOULOU, E., BAKOLAS, A., MOROPOULOU, A., 2019. *Lime putty versus hydrated lime powder: Physicochemical and mechanical characteristics of lime-based mortars*. Constr. Build. Mater. 225, 633–641.

AMBROSI, M., DEI, L., GIORGI, R., NETO, C., BAGLIONI, P., 2001. *Colloidal particles of $Ca(OH)_2$: Properties and applications to restoration of frescoes*. Langmuir 17, 4251–4255.

ANQI, Z., DINGYI, P., 2020. *Rheological experiments on non-Newtonian fluid characteristics of non-colloidal suspensions, in: Chinese Society of Mechanics, Fluid Mechanics Professional Committee*. The 11th National Fluid Mechanics Conference Abstract. (doi.org/Chinese Society of Mechanics, Fluid Mechanics professional committee. The 11th National Fluid Mechanics Conference Abstract)

ARIZZI, A., 2019. *Rheology of lime pastes with biopolymer-based additives*. Mater. Struct. 52, 1–17.

ASGARY, S., NOSRAT, A., SEIFI, A., 2011. *Management of Inflammatory External Root Resorption by Using Calcium-enriched Mixture Cement: A Case Report*. J. Endod. 37, 411–413.

ASIKIN-MIJAN, N., TAUFIQ-YAP, Y.H., LEE, H. V., 2015. *Synthesis of clamshell derived $Ca(OH)_2$ nano-particles via simple surfactant-hydration treatment.* Chemical Engineering Journal 262, 1043–1051.

ATZENI, C., FARCI, A., FLORIS, D., MELONI, P., 2004. *Effect of aging on rheological properties of lime putty* 1766, 1764–1766.

BASTONE, S., CHILLURA, D.F., RENDA, V., LUISA, M., POGGI, G., CAPONETTI, E., 2017. *Alcoholic nanolime dispersion obtained by the insolubilisation-precipitation method and its application for the deacidification of ancient paper*. Colloids Surf. A Physicochem. Eng. Asp. 513, 241–249.

BOHÁ, M., NE, R., 2016. The role of aging on rheological properties of lime putty 151, 34–41.

DARROUDI, M., BAGHERPOUR, M., HOSSEINI, H.A., EBRAHIMI, M., 2016. *Biopolymer-assisted green synthesis and characterization of calcium hydroxide nanoparticles*. Ceram. Int. 42, 3816–3819.

DHANUSKODI, K.K.S., PRABUKUMAR, C.G.S., 2017. *Dielectric and antibacterial studies of microwave assisted calcium hydroxide nanoparticles*. Journal of Materials Science: Materials in Electronics 28, 16509–16518.

GARCÍA-VERA, V.E., TENZA-ABRIL, A.J., MIGUEL, A., LANZÓN, M., 2020. *Calcium hydroxide nanoparticles coatings applied on cultural heritage materials: Their influence on physical characteristics of earthen plasters*. Appl. Surf. Sci. 504, 144195.

HA, H., VU, T., KHAN, M.D., CHILAKALA, R., LAI, T.Q., 2019. *Utilization of lime mud waste from paper mills for efficient phosphorus removal*. Sustainability, 11, 1524.

HUIMIN, W., 2013. *Fundamentals of fluid mechanics*. Tsinghua University Press, Beijing, China.

KANMAZ, F., ALTUNBAS, D., 2022. *Evaluation of the effect of calcium hydroxide paste on sealer penetration into dentinal tubules by confocal laser scanning microscopy*. Aust. Endod. J., 48: 82-90.

KITAMURA, M., KONNO, H., YASUI, A., MASUOKA, H., 2002. *Controlling factors and mechanism of reactive crystallization of calcium carbonate polymorphs from calcium hydroxide suspensions*. J. Cryst. Growth 236, 323–332.

LANZÓN, M., MADRID-MENDOZA, J.A., NAVARRO-MORENO, D., GARCÍA-VERA, V.E., 2023. *Use of eggshell waste: A green and effective method for the synthesis of pure calcium hydroxide suspensions*. Constr. Build. Mater. 377, 131106.

LOUWAKUL, P., SAELO, A., KHEMALEELAKUL, S., 2017. *Efficacy of calcium oxide and calcium hydroxide nanoparticles on the elimination of Enterococcus faecalis in human root dentin* 865–871.

MASCOLO, G., MASCOLO, M.C., VITALE, A., MARINO, O., 2010. *Microstructure evolution of lime putty upon aging*. J. Cryst. Growth 312, 2363–2368.

MASCOLO, M.C., DANIELE, V., MASCOLO, G., 2017. *An approach for a rapid determination of the aging time of lime putty*. Thermochim. Acta 648, 75–78.

NAVRATILOVA, E., NEDELA, V., 2017. *Study of morphological changes of the lime putties during maturing by SEM / ESEM*. Microscopy and Microanalysis, 23(S1).

NAVRÁTILOVÁ, E., TIHLAŘÍKOVÁ, E., NEDĚLA, V., ROVNANÍKOVÁ, P., PAVLÍK, J., 2017. *Effect of the preparation of lime putties on their properties*. Sci Rep, 7, 17260.

PROTECTION, M., 2020. *Superhydrophobic coatings based on siloxane resin and calcium hydroxide nanoparticles for marble protection*. Coatings, 10, 334.

RODRIGUEZ-NAVARRO, C., HANSEN, E., GINELL, W.S., 1998. *Calcium Hydroxide Crystal Evolution upon Aging of Lime Putty* 34, 3032–3034.

RODRIGUEZ-NAVARRO, C., SUZUKI, A., RUIZ-AGUDO, E., 2013. *Alcohol dispersions of calcium hydroxide nanoparticles for stone conservation*. Langmuir, 29, 11457–11470.

ROMERO-HERMIDA, M.I., BORRERO-LÓPEZ, A.M., ALEJANDRE, F.J., FLORES-ALÉS, V., SANTOS, A., FRANCO, J.M., ESQUIVIAS, L., 2019. *Phosphogypsum waste lime as a promising substitute of commercial limes: A rheological approach*. Cem. Concr. Compos. 95, 205–216.

RUIZ-AGUDO, E., RODRIGUEZ-NAVARRO, C., 2010. *Microstructure and rheology of lime putty*. Langmuir, 26, 3868–3877.

SAMANTA, A., CHANDA, D.K., DAS, P.S., GHOSH, J., KUMAR, A., DEY, A., 2016. *Synthesis of nano calcium hydroxide in aqueous medium*. J. Am. Ceram. Soc., 99:795.

SHIN, H.G., KIM, H., KIM, Y.N., LEE, H.S., 2009. *Preparation and characterization of high surface area calcium hydroxide sorbent for SO_2 removal*. Current Applied Physics 9, S276–S279.

SY, K., AGOSSA, K., MATON, M., CHIJCHEAPAZA-FLORES, H., MARTEL, B., SIEPMANN, F., DEVEAUX, E.,

BLANCHEMAIN, N., NEUT, C., 2021. *How Adding Chlorhexidine or Metallic Nanoparticles Affects the Antimicrobial Performance of Calcium Hydroxide Paste as an Intracanal Medication: An In Vitro Study*.

TAGLIERI, G., MONDELLI, C., DANIELE, V., PUSCEDDU, E., SCOCCIA, G., 2014. *Synthesis, textural and structural properties of calcium hydroxide nanoparticles in hydro-alcoholic suspension*. Advances in Materials Physics and Chemistry 04, 50–59.

WANG, X., WEI, M., LIU, K., CUI, K., YANG, Y., TIAN, Z., 2024. *Particle Size of Calcium Hydroxide Prepared by Wet Digestion: Influencing Factors and Mechanism* 2300335, 1–11.

WEIFEI, Z., 2004. *Experimental study of operating parameters of lime slaking process and dissolution rate of calcium hydroxide*. Zhejiang University.

WENLI, Y., 2021. *Study on the preparation of calcium hydroxide and its carbonated product performance*. East China University of Science and Technology.

XIN, W., MING, W., KUN, L., 2023. *Progress in preparation technology and application of special kinds of calcium hydroxide*. Modern Chemical Industry, 26–30.

YONG, L.L., PERERA, S.V.A.D.N.J., SYAMSIR, A., EMMANUEL, E., PAUL, S.C., ANGGRAINI, V., 2019. *Stabilization of a residual soil using calcium and magnesium hydroxide nanoparticles: a quick precipitation method*. Applied Sciences, 9(20), 1–15.